Effect of Zinc Ions on tRNA Structure: Imino Proton NMR Spectroscopy†

John M. Flanagan‡,§ and K. Bruce Jacobson*,‖

University of Tennessee—Oak Ridge Graduate School of Biomedical Sciences and Biology Division, Oak Ridge National Laboratory, Oak Ridge, Tennessee 37831

Received March 11, 1988

ABSTRACT: The structure of tRNA in solution was explored by NMR spectroscopy to evaluate the effect of divalent cations, especially zinc, which has a profound effect on the chromatographic behavior of tRNAs in certain systems. The divalent ions Mg^{2+} and Zn^{2+} have specific effects on the imino proton region of the ^1H NMR spectrum of valine transfer RNA ($tRNA^{Val}$) of *Escherichia coli* and of phenylalanine transfer RNA ($tRNA^{Phe}$) of yeast. The dependence of the imino proton spectra of the two tRNAs was examined as a function of Zn^{2+} concentration. In both tRNAs the tertiary base pair (G-15)·(C-48) was markedly affected by Zn^{2+} (shifted downfield possibly by as much as 0.4 ppm); this is the terminal base pair in the augmented dihydrouridine helix (D-helix). Base pair (U-8)·(A-14) in yeast $tRNA^{Phe}$ or (s^4U-8)·(A-14) in $tRNA_1^{Val}$, which are stacked on (G-15)·(C-48), was not affected by Zn^{2+}, except when 1–2 Mg^{2+} ions per tRNA were also present. Another imino proton that may be affected by Zn^{2+} in both tRNAs is that of the tertiary base pair (G-19)·(C-46). The assignment of this resonance in yeast $tRNA^{Phe}$ is tentative since it is located in the region of highly overlapping resonances between 12.6 and 12.3 ppm. This base pair helps to anchor the D-loop to the TΨC loop. Surprisingly, the imino proton of (G-18)·(Ψ-55) is not similarly affected by Zn^{2+}, indicating that the effect of Zn^{2+} is not on G-57 which is the central non-hydrogen-bonded base in the "guanosine sandwich" created by the stacking of G-19, G-57, and G-20. The solution structure of $tRNA^{Phe}$ shows marked correlation to the crystal structure in terms of Zn^{2+} interactions [Rubin, J. R., Wang, J., & Sundaralingam, M. (1983) *Biochim. Biophys. Acta 756*, 111–118].

The low-field ^1H NMR spectra of tRNAs contain resonances corresponding to hydrogen-bonded imino protons of the helical stems and tertiary base pairs [for review, see Reid (1981)]. Each hydrogen-bonded imino proton gives rise to a separate resonance, the chemical shift of which is predominately influenced by ring-current effects of neighboring base pairs. The imino proton spectrum is thus particularly sensitive to the orientation and distances between neighboring base pairs (Arter & Schmidt, 1976).

The imino proton spectrum of yeast $tRNA^{Phe}$ has been assigned independently by two groups using the sequential nuclear Overhauser effects (NOE) technique (Roy & Redfield, 1982; Heerschap et al., 1982, 1983a,b). This region of the *Escherichia coli* $tRNA_1^{Val}$ spectrum has also been completely assigned both by sequential NOE (Hare & Reid, 1982) and more recently by a two-dimensional NOE technique (Hare et al., 1985).

Studies on the effect of Zn^{2+} on tRNA structure are hampered by the fact that Zn^{2+}, like Pb^{2+}, catalyzes the alkaline hydrolysis of RNA at neutral pH (Farkas, 1968; Butzow & Eichhorn, 1975; Werner et al., 1976; Sundaralingam et al., 1984). The hydrolysis of RNA by metal ions is not limited to Pb^{2+} and Zn^{2+}; even Mg^{2+} will degrade RNA, although the rate of this reaction is much less than that for either Pb^{2+} or Zn^{2+} (Wintermeyer & Zachau, 1973; Werner et al., 1976). The degradation of RNA by these metals can be suppressed by lowering the pH below 6.0, apparently without affecting their sites of interactions (Brown et al., 1985).

In this study we have investigated the specific effects of metal ions on the structure of *E. coli* $tRNA_1^{Val}$ and yeast $tRNA^{Phe}$ by ^1H NMR spectroscopy. These experiments were prompted by the observations of Hiatt and Jacobson (1981) and Flanagan and Jacobson (1987) that Zn^{2+} has a unique effect on tRNA structure as judged by the increased retention of tRNAs when Zn^{2+} was present during RPC-5 chromatography. *E. coli* $tRNA_1^{Val}$ is particularly suited for imino proton NMR studies because of the high degree of resolution observed for resonances in this region.

Materials and Methods

Yeast $tRNA^{Phe}$ was purchased from Boehringer Mannheim Biochemical Co.; it had an amino acid acceptance of 1460 pmol/A_{260} as determined by the manufacturer. *E. coli* $tRNA_1^{Val}$ was purchased from Subriden RNA (P.O. Box 121, Rolling Bay, WA 98061). In all but the initial experiments with $tRNA^{Phe}$, the residual 1 to 2 Mg^{2+} ions were removed by dissolving the tRNA (7–10 mg) in 10 mL of 10 mM EDTA at pH 7.0 and heating it at 60 °C for 5 min. This solution was allowed to return to room temperature and then vacuum dialyzed against distilled water to a final volume of 0.25 mL and lyophilized. For the NMR studies, ~8 mg of the lyophilized tRNA was dissolved in 0.3 mL of buffer containing 500 mM NaCl and 10 mM NaOAc, pH 4.6. A 50-μL aliquot of D_2O was added as a signal lock, and 0.2 mM 4,4-dimethyl-4-silapentane-1-sulfonate (DSS) was added as an internal reference. The final concentration of tRNA was 1 mM. Divalent metal ions were added (Mg^{2+} or Zn^{2+}) in the choride form by transferring the tRNA sample to a clean piece of Parafilm and then adding aliquots of the stock metal solutions.

Proton NMR spectra were collected in the laboratory of B. Reid (University of Washington) on a Bruker WM 500 FT NMR spectrometer with a 16-bit digitizer resolution, using

† This research was jointly sponsored by NIH Training Grant GM 07438 (J.M.F.) and by the Office of Health and Environmental Research, U.S. Department of Energy, under Contract DE-AC05-84OR21400 with Martin Marietta Energy Systems, Inc.

* Address correspondence to this author.

‡ University of Tennessee—Oak Ridge Graduate School of Biomedical Sciences.

§ Department of Molecular Biophysics and Biochemistry, Yale University, 260 Whitney Ave., P.O. Box 6666, New Haven, CT 06511.

‖ Oak Ridge National Laboratory.

0006-2960/88/0427-5778$01.50/0

a modified 21412 Redfield pulse sequence (Redfield, 1978). The spectra were collected in 8K data channels with a sweep width of 1400 Hz, a pulse length of 205 μs, and a carrier offset of 4730 Hz downfield of water. Typically, 1000 scans were collected for each sample.

Nuclear Overhauser effects (NOEs) were measured by collecting sets of 16 scans with the decoupler alternately on- and off-resonance. Typically, 4000 scans were collected for each experiment. Saturation pulses between 0.4 and 1.5 s were used; the decoupler power was adjusted to just saturate the target resonance with minimal spillover to neighboring peaks. The long saturation pulse (1.5 s) was used to facilitate observation of spatially distant protons via second-order NOEs which can be observed under these conditions.

RESULTS

Effect of Zn^{2+} on the Imino Proton Spectra of E. coli $tRNA^{Val}$. Under optimal solvent conditions for the ^1H NMR spectrum of *E. coli* $tRNA^{Val}$, 22 peaks corresponding to 27 protons can be resolved (Hare et al., 1985), allowing a detailed examination of metal ion effects on tRNA structure. The cloverleaf representation of *E. coli* $tRNA_1^{Val}$ is

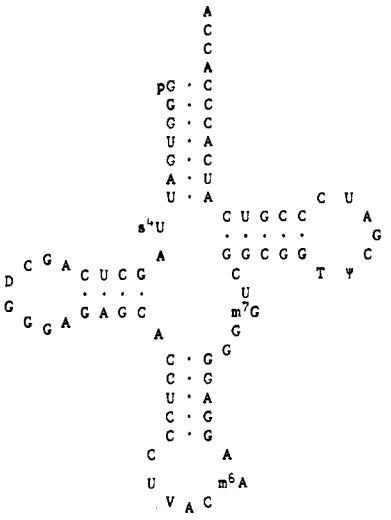

$tRNA^{Val}$

The anticodon stem of this tRNA could not be completely assigned since it is symmetric about the central base pair, A·U-29; hence, the assignment of base pairs 27, 31 and 28, 30 cannot be obtained independently (Hare et al., 1985).[1]

NMR spectra of $tRNA^{Val}$ were obtained in 500 mM NaCl and 10 mM NaOAc buffer, pH 4.6, containing various concentrations of added Zn^{2+} (Figure 1). The Mg^{2+} content of these samples was <0.1 (Hyde & Reid, 1985a). The imino proton resonances were designated from A to Z after Hare and Reid (1982). The sample containing no Mg^{2+} (Figure 1a) is qualitatively similar to spectra obtained with no Mg^{2+} at pH 7.0 and 360 MHz [Figure 2a of Reid et al. (1979)] and spectra obtained under similar conditions at 500 MHz (Hare and Reid, personal communication). There are several notable exceptions particularly in the regions between 14 and 12.5 ppm. The assignments of these resonances will be discussed below.

Addition of Zn^{2+} primarily affects four resonances: C, L′, R, and T′ (Figure 1). All four of these resonances are progressively shifted downfield with increasing Zn^{2+} concentrations. Two other resonances originating from peak O are also affected by Zn^{2+}, although only at concentrations above 4 mM. Figure 2 summarizes the changes in chemical shifts for all the imino protons in this region due to Zn^{2+}.

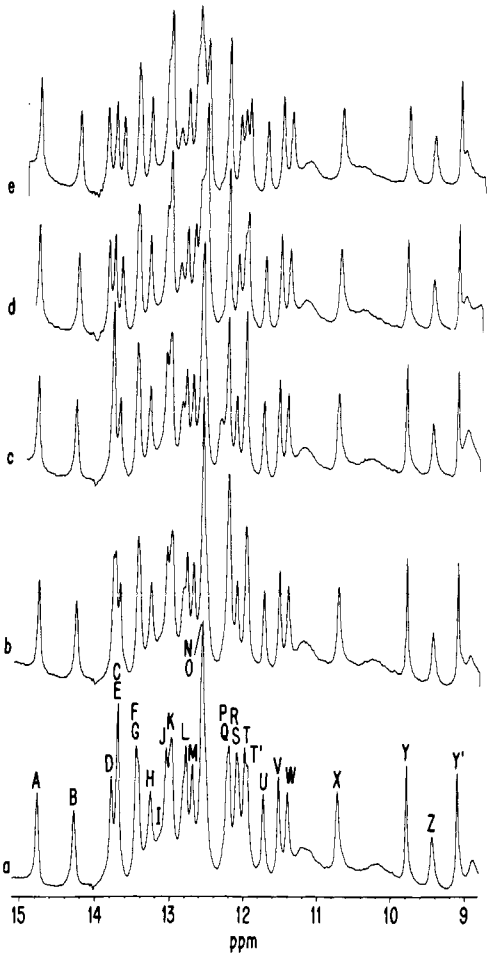

FIGURE 1: Effect of increasing concentrations of Zn^{2+} on the low-field NMR spectra of 1 mM *E. coli* $tRNA_1^{Val}$. The tRNA spectra were collected at 35 °C in a buffer containing 500 mM NaCl and 10 mM NaOAc, pH 4.6. (a) 0, (b) 2, (c) 4, (d) 6, and (e) 8 mM added $ZnCl_2$.

The largest change in chemical shift was seen for peak R, located at 12.1 ppm in the absence of divalent cations. This resonace is shifted downfield by 0.6 ppm to 12.7 ppm upon addition of 8 mM Zn^{2+}. The effect of Zn^{2+} on peak R did not appear to be linear. The two protons which are believed to resonate under peak RS in the absence of divalent ions are G·C-49 and the tertiary base pair (G-15)·(C-48).

To determine which of these protons is affected by Zn^{2+}, we examined the NOE connectivity of peak A, (s^4U-8)·(A-14), in the presence of 7 mM Zn^{2+}, which is spatially near (G-15)·(C-48) (Figure 3a). Although these two base pairs are adjacent, the distance between imino protons approaches the limit of detection for a first-order NOE (~5 Å). To increase our chances of observing an NOE to (G-15)·(C-48), we decreased the temperature to 17 °C and used a 1.5-s saturation pulse. Under these conditions some second-order NOEs can be observed. Presaturation of A, (s^4U-8)·(A-14), gives rise to NOEs at ~13.1, 8.6, 12.7, and possibly 13.3 ppm. The strong NOE to the aromatic proton region (8.6 ppm) shows that peak A is due to an A·U base pair. The relatively large NOE at 13.1 ppm is in the region where the imino proton of G·C-13 is thought to resonate. Since the imino proton from this base pair is believed to be closer to (s^4U-8)·(A-14) than to (G-15)·(C-48), it is resonable to conclude that the NOE

[1] Abbreviations: Y, wybutine; Ψ, pseudouridine; s^4U, 4-thiouridine; D, dihydrouridine.

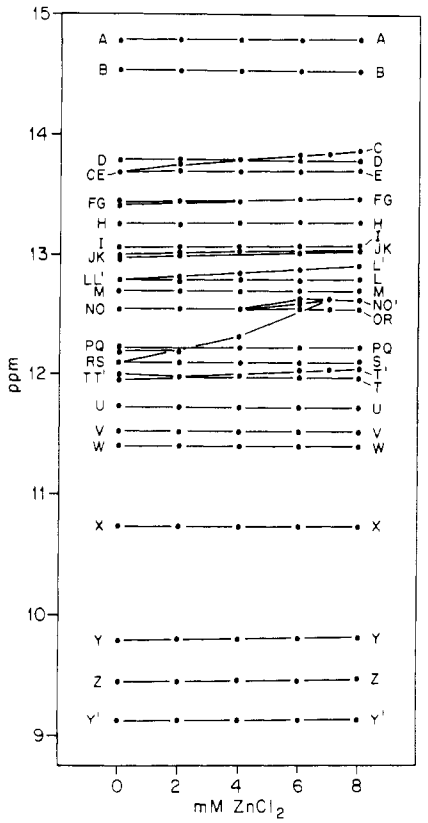

FIGURE 2: Summary of chemical shifts of peaks in Figure 1 at various concentrations of zinc.

at 13.1 ppm is due to G·C-13. The weak NOE at 12.7 ppm is probably a second-order effect. The next closest imino proton to (s^4U-8)·(A-14) is that of G-15; thus, we believe that the NOE to 12.7 ppm (peak R) is due to the imino proton of (G-15)·(C-48). Hare et al. (1985) performed a similar experiment and showed that (G-15)·(C-48) resonated at ~12.1 ppm (peak RS), in the absence of divalent cations at pH 7.0. Using this information, we conclude that the presence of Zn^{2+} shifts the imino proton of (G-15)·(C-48) to lower field strengths.

Peak C of $tRNA_1^{Val}$ is also affected by Zn^{2+}. Its chemical shift increases linearly with increasing Zn^{2+} concentrations. In 8 mM Zn^{2+} this proton resonates 0.17 ppm downfield from its position in the absence of Zn^{2+} (Figure 2). In fact, in 6 mM Zn^{2+} peaks C, D, and E are resolved into three single proton peaks.

To determine which of these protons are affected by Zn^{2+}, we examined the NOE connectivity of the most upfield of these protons in 7 mM Zn^{2+}, peak E (Figure 3b). Previously, Hare et al. (1985) assigned five imino protons to this general region (14.0–13.4 ppm, CDEFG). The imino protons assigned here were the A·U base pairs U·A-12, U·A-29, and U·A-4, the A·T base pair [(T-54)·(A-58)], and G·C-11. To determine which of these resonances were perturbed by Zn^{2+}, we examined the NOE connectivity of peak E at 12.7 ppm (Figure 3b). If E was due to an A·U or an A·T base-pair, there should be a strong NOE to the aromatic region (7–9 ppm). Since we did not observe an NOE to this region, we believe that peak E is due to a G·C base pair, G·C-11. Irradiation of E also produces what appears to be a NOE to peak O. Four resonances have been assigned to peak O: G·C-2, U·A-7, G·C-10, and C·G-31 (Hare et al., 1985). An NOE to peak O would thus lend support to our assignment of peak E, since of the five imino protons which resonate in peaks CDEFG only G·C-11 is expected to give rise to this NOE. However, since peak O contains several protons, it is by no means conclusive evidence.

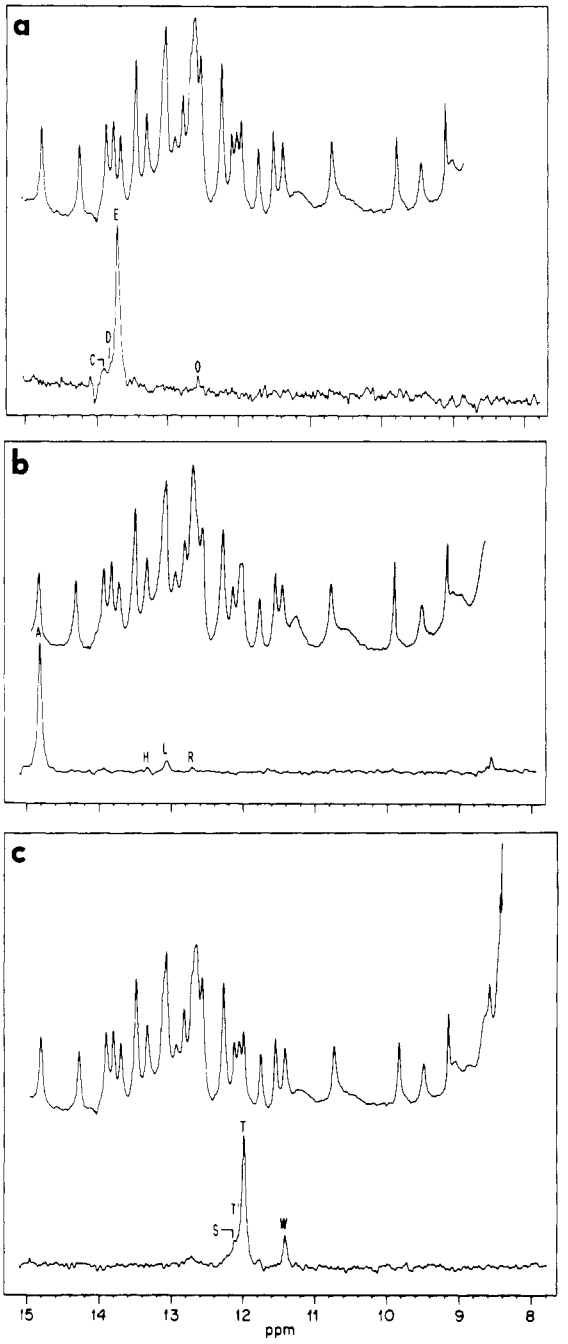

FIGURE 3: One-dimensional NOEs of $tRNA_1^{Val}$. (a) Selective saturation (1.5 s) of peak A (Figure 1). The sample contains 1 mM *E. coli* $tRNA_1^{Val}$, 500 mM NaCl, 10 mM NaOAc, pH 4.6, and 7 mM $ZnCl_2$ at 17 °C. (b) Selective saturation (0.4 s) of peak E (Figure 1). The sample and conditions were identical with those used in (a) except that the temperature was 37 °C. (c) Selective saturation (0.4 s) of peak T. The sample and conditions were the same as that used in (a).

The assignment of peak C is complicated by the fact that both peaks C and D are affected by irradiation of E. We suggest that D arises from direct irradiation spillover from E and that C is due to an NOE from C·G-11 (peak E) and is the imino proton of U·A-12. Two indirect pieces of evidence support these assignments: (a) a similar effect of Zn^{2+} is seen in yeast $tRNA^{Phe}$ (peak D see below) (this is due to either C·G-11, U·A-12, or U·A-52, but not U·A-29); (b) from the crystal structure of yeast $tRNA^{Phe}$ in the presence of Zn^{2+} (Rubin et al., 1983), there is no Zn^{2+} binding site near U·A-29 while U·A-12 is very close to the strongest Zn^{2+} binding site.

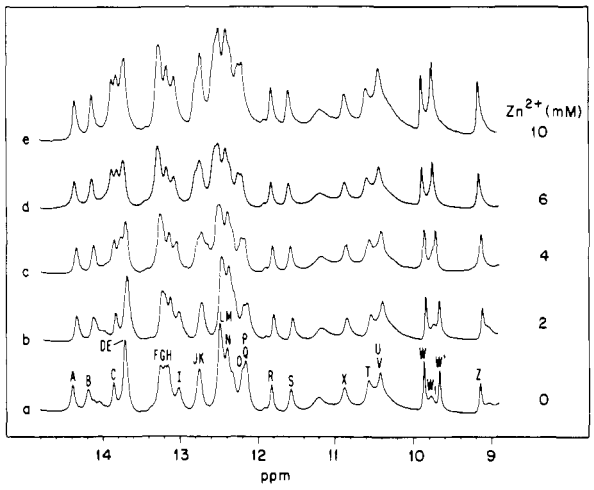

FIGURE 4: Effect of increasing concentrations of Zn^{2+} on low-field NMR spectra of 1 mM yeast $tRNA^{Phe}$. Conditions were as for Figure 1a. (a) 0, (b) 2, (c) 4, (d) 6, and (e) 10 mM added $ZnCl_2$.

No one piece of evidence is conclusive although the evidence, taken together, supports the assignments of peak C to U·A-12, D to U·A-29, and E to G·C-11 in *E. coli* $tRNA_1^{Val}$.

The presence of Zn^{2+} also causes one proton to shift downfield from peak L (12.8 ppm) to L′ (12.9 ppm). The imino protons of G·C-53 and (G-19)·(C-56), a tertiary base pair, are assigned to this region (Hare et al., 1985). We cannot determine directly which of these two protons is affected; neither of the spatially nearby base pairs of G·C-53, namely, peaks F [(T-54)·(A-58)] and P (G·C-13), are affected by Zn^{2+}. While for (G-19)·(C-56) only its 5′ neighbor peak X [(G-18)·(Ψ-55)] can be monitored directly, it too appears to be unaffected by Zn^{2+}. The 3′ neighbor of (G-19)·(C-56) is G-20; the imino proton of this base should not give rise to a resonance in this region.

Here, as in the previous two cases, we must resort to ancillary data to tentatively assign peak L′. In yeast $tRNA^{Phe}$, Zn^{2+} has been shown to bind to the phosphate oxygen of G-19, while no Zn^{2+} binds near G·C-53 (Rubin et al., 1983). We therefore tentatively assign the component of L/L′ affected by Zn^{2+} to (G-19)·(C-56).

Zn^{2+} also shifts peak T′ downfield. The two protons which resonate in this region are the imino protons of G·C-1 and U-64, which is involved in a base pair interaction with G-50. The imino proton of G-50, peak W, is unaffected by Zn^{2+}, suggesting that the imino proton of G·C-1 is the mobile proton. To test this, we presaturated peak T in 8 mM Zn^{2+}; under these conditions peak T at 12.0 ppm contains only a single proton (Figure 3c). We observed a strong NOE to peak W, the imino proton of G-50, suggesting that peak T is due to U-64, while the mobile proton, peak T′, is due to G·C-1.

Presaturation of peak T also gave rise to two other NOEs, one at 12.8 ppm and another at 12.1 ppm. The peak at 12.8 ppm is probably due to G·C-51, the 3′ neighbor of U-64. The NOE to 12.1 ppm, peak S, may in fact be due to direct irradiation spillover, although spillover to the central peak, T′, does not appear to be large. If this is an authentic NOE, it would confirm our earlier assignment of peak S to G·C-49, the 5′ neighbor of (G-50)·(U-64).

The assignment of G·C-1 to the mobile proton of TT′ may help explain the effect of Zn^{2+} on peak NO′ (Figures 1 and 2). Two protons in NO′ are perturbed by Zn^{2+}; one is believed to be G·C-10 while the other cannot be assigned. The imino protons which are thought to resonate near NO′ are U·A-7, G·C-2, and G·C-10. G·C-2 is spatially located next to G·C-1 (peak T′), which is affected by Zn^{2+}, and it too may be so

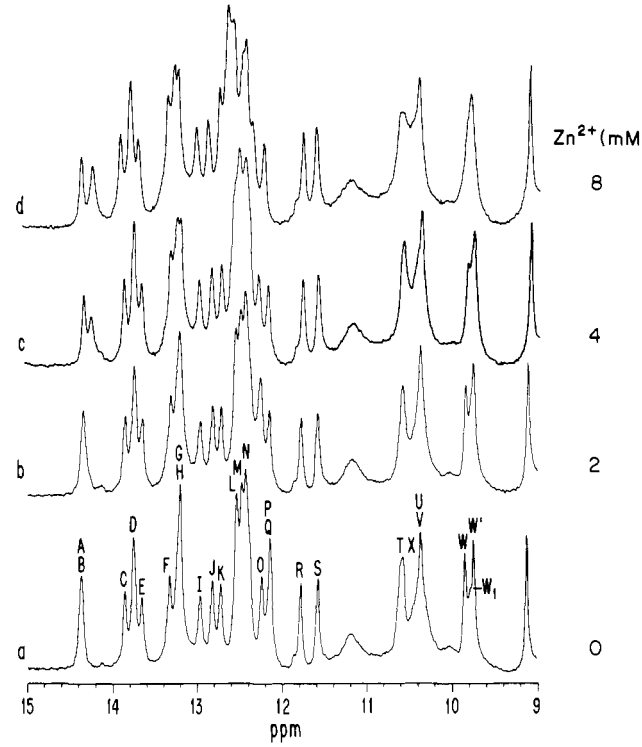

FIGURE 5: Effect of Zn^{2+} on the low-field NMR spectra of 1 mM yeast $tRNA^{Phe}$ after removal of residual Mg^{2+}. Conditions for removal of residual Mg^{2+} are described under Materials and Methods. (a) 0, (b) 2, (c) 4, (d) 6, and (e) 10 mM added $ZnCl_2$.

affected. However, at least one of the components of NO′ is affected only at concentrations of Zn^{2+} above 4 mM, while Zn^{2+} affects G·C-1 at all concentrations.

Yeast $tRNA^{Phe}$: Effect of Removal of Divalent Cation on the Imino Proton ^1H NMR Spectrum. The cloverleaf representation of yeast $tRNA^{Phe}$ is (RajBhandry et al., 1981)

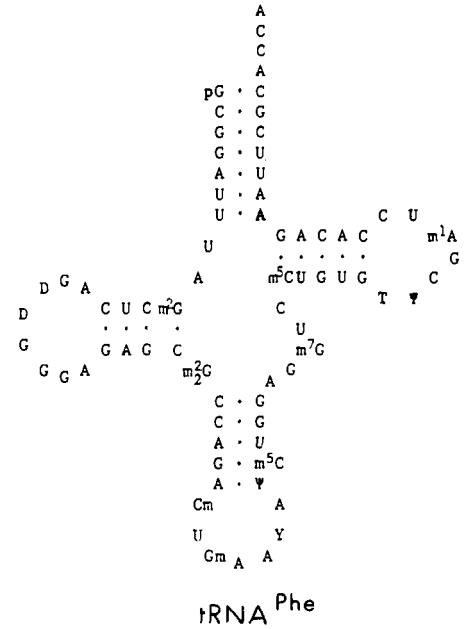

The imino proton spectra collected in the presence of 1–2 Mg^{2+} and after rigorous removal of Mg^{2+} are shown in Figures 4a and 5a, respectively. Removal of Mg^{2+} affected most of the residues in the region between 9 and 15 ppm. The imino proton resonances are lettered A–Z in accordance with Heerschap et al. (1982).

The magnitudes of the chemical shift changes ranged from 0 to 0.4 ppm due to the removal of Mg^{2+}. The imino proton

Table I: Summary of Chemical Shifts in $tRNA^{Phe}$ That Are Affected by the Presence of Mg^{2+}

		resonances (ppm)				
				Heerschap et al.		
base pair	peak	1–2 Mg^{2+} per tRNA[a]	~0 Mg^{2+} per tRNA[b]	buffer 1[c]	buffer 2[d]	Roy and Redfield[e]
(A-6)·(U-67)	A	14.40	14.40	14.40	14.46	14.35
(A-8)·(U-14)	B	14.40	14.18	14.40	14.20	14.20
(U-52)·(A-62)	D	13.72	13.69	13.80	13.73	13.70
(U-12)·(A-23)						
(T-54)·(m^1A-58)						
(C-11)·(G-24)	E	13.65	13.69	13.65	13.73	13.70
(G-1)·(C-72)	J	12.80	12.76	12.84	12.78	
(m^2G-10)·(C-25)	K	12.70	12.76	12.74	12.77	12.75
NH-1 (Ψ-55)	X	10.89	10.05	11.00	10.48	11.00

[a] Buffer: 500 mM NaCl, 10 mM NaOAc, pH 4.6, at 35 °C. [b] Buffer: 500 mM NaCl, 10 mM NaOAc, pH 4.6, tRNA sample treated as in Hyde and Reid (1985) to remove residual Mg^{2+}, at 35 °C. [c] Buffer 1: 80 mM NaCl, 30 mM cacodylate, pH 7.0, 5 mM $MgCl_2$, 0.1 mM EDTA, at 23 °C. [d] Buffer 2: 400 mM NaCl, 30 mM cacodylate, pH 7.0, 0.2 mM EDTA (residual Mg^{2+} <0.01 equiv), at 23 °C. [e] Buffer: 100 mM NaCl, 10 mM phosphate, pH 7.0, 1 mM EDTA, at 20 °C.

resonances most affected are summarized in Table I. Included for comparison are the assignments and chemical shifts for these peaks determined by Heerschap et al. (1983b) and Roy and Redfield (1982). Interestingly, the imino proton chemical shifts for yeast $tRNA^{Phe}$ in the sample containing residual Mg^{2+} (Figure 4a) was very similar to that obtained by Heerschap et al. (1982, 1983a,b) in their buffer 1 (80 mM NaCl, 30 mM cacodylate, pH 7.0, 5 mM $MgCl_2$, 0.1 mM EDTA) while our zero Mg^{2+} (Figure 5a) sample resembled the no Mg^{2+} sample of Roy and Redfield (1982). For yeast $tRNA^{Phe}$, mildly acid conditions appeared to have little apparent effect on the imino proton spectra. These are consistent with the results of an earlier study by Wong et al. (1973) at 360 MHz which concluded that no gross spectral changes accompanied lowering the pH to 4.6.

Titration of Yeast $tRNA^{Phe}$ with Zn^{2+}. The imino proton spectra of yeast $tRNA^{Phe}$ are shown as a function of increasing concentrations of added Zn^{2+} (Figure 4), and the data are summarized in Figure 6. In addition to added Zn^{2+}, the tRNA samples contained 1–2 residual Mg^{2+} ions per tRNA. The addition of Zn^{2+} perturbs a number of resonances with peaks B, M, and P experiencing the largest effects. Peaks M and P are shifted downfield, while B moves upfield. Although the effects of Zn^{2+} on peaks P and B are in different directions, both appear to reach completion at about 4 mM Zn^{2+}.

Here, as in earlier work with Mg^{2+} (Hyde & Reid, 1985b), the effect of metal ions is seen in all the stem structures of the tRNA; however, most effects appear to be very local; even protons of the same base can be affected differently (Tropp & Redfield, 1981). We have observed only one case where neighboring base pairs, represented by peaks B and P, appear to be affected in tandem by Zn^{2+}.

Peak B shifts upfield by 0.13 ppm and is assigned to (U-8)·(A-14), while P shifts 0.25 ppm downfield and has been assigned to (G-15)·(C-48). As suggested above, both of these effects appear to be complete at 4 mM Zn^{2+}. Peak I, due to G·C-13, which is stacked on (U-8)·(A-14), is unaffected. (G-15)·(C-48) is the terminal base pair in the augmented D-helix and would not be expected to affect any other resonance in this region.

Effect of Zn^{2+} on $tRNA^{Phe}$ Imino Proton Resonances in the Absence of Mg^{2+}. Figure 5 shows the imino proton spectra of yeast $tRNA^{Phe}$ at varying concentrations of added Zn^{2+}. The residual Mg^{2+} content of these samples was <0.1 equiv of Mg^{2+} per tRNA. Figure 7 summarizes the effects of Zn^{2+} on this region. Under these conditions the largest effects of Zn^{2+} are seen on peaks D, L_1, and P, all of which are shifted downfield. For each of these three peaks the effects are observed even at the lowest Zn^{2+} concentration.

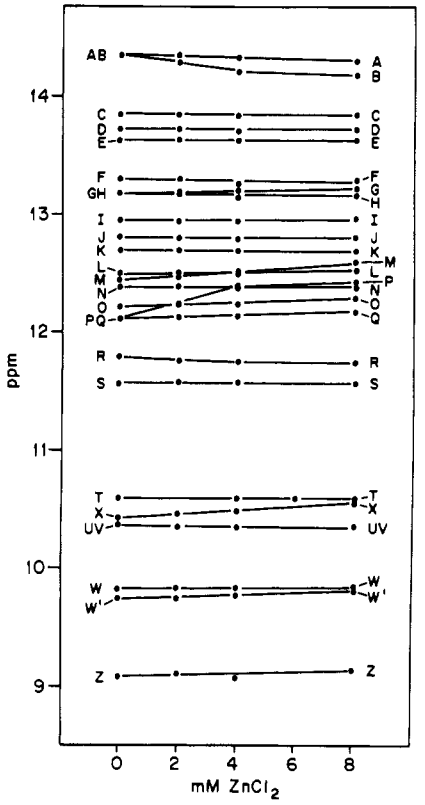

FIGURE 6: Summary of chemical shifts of peaks in Figure 4 at various concentrations of zinc.

By far the largest effect of Zn^{2+} is seen on peak P. In the absence of divalent cations, peaks P and Q correspond to a single peak of two protons. The addition of Zn^{2+} shifts one proton downfield into the highly overlapped region between 12.6 and 12.4 ppm. This resonance is probably the same one affected by Zn^{2+} in the presence of Mg^{2+}, peak P in Figures 4 and 6. We have tentatively assigned the mobile proton of P to the imino proton of (G-15)·(C-48). This imino proton is also affected by Zn^{2+} in $tRNA^{Val}$, peak R in Figures 1 and 2. In all three cases the effect of Zn^{2+} on this resonance was relatively large (possibly as much a 0.5 ppm in $tRNA_1^{Val}$). The exact magnitude of the change in chemical shift for peak P of $tRNA^{Phe}$ cannot be determined because of the lack of resolution in this region of the spectrum.

Another relatively large downfield shift (~0.2 ppm) was seen for peak L_1 (Figures 5 and 7). One proton from the LMN grouping shifts into peak K. Numerous imino protons are believed to resonate under LMN including C·G-43, G·C-30, (G-19)·(C-56), C·G-2, m^5C·G-49, G·C-53, G·C-51, and

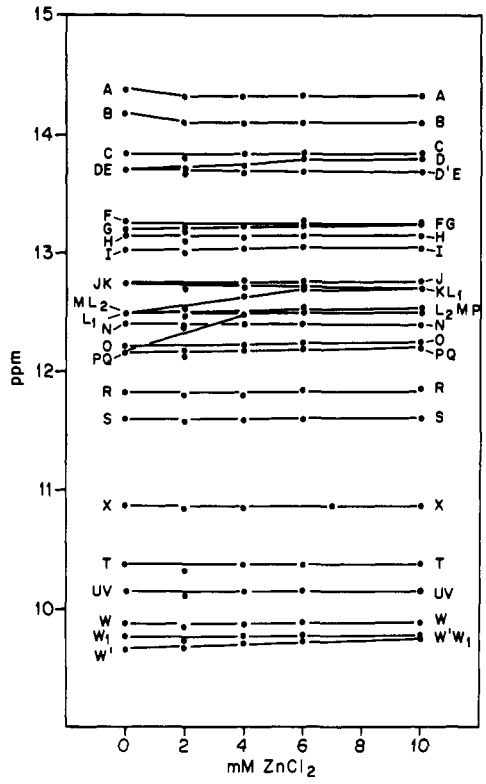

FIGURE 7: Summary of chemical shifts of peaks in Figure 5 at various concentrations of zinc.

possibly (T-54)·(m^{1}A-58) (Heerschap et al., 1982, 1983a,b; Roy & Redfield, 1982). Without supporting NOE data, it is not possible to draw any conclusion about the imino proton which gives rise to peak L_1.

Addition of 10 equiv of Zn^{2+} per tRNA causes one proton to be shifted downfield from peak DE to 13.8 ppm (Figures 5 and 7). The imino protons that resonate under DE are U·A-12, U·A-52, and C·G-11. Base pair U·A-12 is involved in a tertiary interaction with the amino group of A-9, the upfield component of WW_1W' at 9.7 ppm (Choi & Redfield, 1985); this peak is also affected by Zn^{2+}, suggesting that the component of D affected by Zn^{2+} is U·A-12. However, the amino proton of A-9 is also affected by Zn^{2+} when 1–2 Mg^{2+} are present, and no component of D is similarly affected (Figures 4 and 6). U·A-12 appears to be affected by Zn^{2+} in $tRNA^{Val}$ (Figures 1, 2, and 3a), which may lend some support to the assignment of this proton as the mobile one in $tRNA^{Phe}$.

The presence of residual Mg^{2+} affects the imino proton spectra of yeast $tRNA^{Phe}$ obtained in the absence or presence of Zn^{2+}. The spectrum of yeast $tRNA^{Phe}$ in the presence of 10 mM Zn^{2+} with no Mg^{2+} (Figure 5) is significantly different than the spectrum obtained with 8 mM Zn^{2+} and 1–2 mM Mg^{2+} (Figure 4). In the latter, one proton in the group of peaks labeled TXUV (Figure 4) appears to be displaced downfield by the addition of Zn^{2+}. When no Mg^{2+} is present however, the addition of Zn^{2+} has little effect on this proton. These observations suggest that this proton is not sensitive to Zn^{2+}, although it may be affected by Mg^{2+}.

The presence of Mg^{2+} influences how Zn^{2+} affects the resolution of peak WW′. In the absence of divalent ions, peaks W and W′ are separated by 0.2 ppm (Figure 5); with 10 mM Zn^{2+} they are separated by 0.12 ppm, primarily by shifting peak W′ downfield (Figure 5). In the presence of 1–2 Mg^{2+} ions per tRNA, peaks W and W′ are separated by 0.12 ppm (Figure 4); the addition of 8 mM Zn^{2+} causes the resolution to deteriorate further to give an asymmetric peak for WW′, suggesting that they are separated only slightly (Figure 4). Peak W′ has been assigned to the amino proton of A-9, which participates in a tertiary interaction with U·A-12 (Choi & Redfield, 1985).

Table II: Summary of the Imino Proton Resonances in Yeast $tRNA^{Phe}$ and *E. coli* $tRNA_1^{Val}$ That Are Affected by the Presence of Zn^{2+}

$tRNA^{Phe}$				$tRNA^{Val}$ (no Mg present)	
1–2 Mg^{2+}		no Mg^{2+} present			
peak	assignment	peak	assignment	peak	assignment
B	(U-8)·(A-14)				
		D	(U-12)·(A-23)	C	(U-12)·(A-23)
G	?	G	?		
M	(G-19)·(C-56)	L′	(G-19)·(C-56)	L′	(G-19)·(C-56)
				N[a]	(G-2)·(C-71)
		K	(G-10)·(C-25)	O[a]	(G-10)·(C-25)
P	(G-15)·(C-48)	P	(G-15)·(C-48)	R	(G-15)·(C-48)
				T	(G-1)·(C-72)
X	N1-H of Ψ-55				
W′	amino-proton of A-9	W′	amino proton of A-9		

[a] This effect appears only above 4 mM Zn^{2+}.

Because of the highly overlapped nature of the resonances in the yeast $tRNA^{Phe}$ imino proton spectrum, especially in the absence of Mg^{2+}, a great deal of potentially interesting data is lost. This is especially true in the region between 12.4 and 12.0 ppm where Zn^{2+} appears to have a number of interesting effects.

Discussion

One effect Zn^{2+} has on tRNA structure is to alter the sites on the tRNA available for interaction with RPC-5 columns (Hiatt & Jacobson, 1980; Flanagan & Jacobson, 1987). The nature of this alteration is not, as yet, completely understood. One explanation for the aberrant chromatographic behavior is that Zn^{2+} disrupts the hydrogen-bonded structure of tRNA, allowing 8–10 previously "hidden" negative charges to interact with the column. Clearly, this is not the case since the number of resonances in the imino proton spectra of both $tRNA^{Phe}$ and $tRNA^{Val}$ is the same in the presence and absence of Zn^{2+}. It is argued elsewhere (Flanagan & Jacobson, 1987) that hydrophobic forces play a role in the increased retention of tRNA on RPC-5 due to Zn^{2+}. The basis of these conclusions, as well as the nature of some possible Zn^{2+} binding sites in solution, will be discussed in light of the known structure of $tRNA^{Phe}$ in the presence of Zn^{2+} as deduced from the present NMR study and from X-ray diffraction (Rubin et al., 1983).

In Table II we summarize the zinc-induced changes in the imino proton spectra of yeast $tRNA^{Phe}$ in the presence of 1–2 equiv of Mg^{2+} ions and also of $tRNA^{Phe}$ and *E. coli* $tRNA_1^{Val}$ in the absence of Mg^{2+}. Zn^{2+} affects both tRNAs similarly, with the majority of effected resonances occurring in the D-arm. In all three experiments, Zn^{2+} had its largest effect on the imino proton of (G-15)·(C-48), a reversed Watson–Crick-type base pair that forms the base of the augmented D-helix. In the absence of Mg^{2+} the base pair (U-8)·(A-14) in $tRNA^{Phe}$ and (s^{4}U-8)·(A-14) in $tRNA^{Val}$, which is spatially adjacent to (G-15)·(C-48), are not affected by Zn^{2+}. The observations suggest that Zn^{2+} interacts specifically near or on (G-15)·(C-48) in solution.

The imino proton of (G-19)·(C-56) like that of (G-15)·(C-48) is affected by Zn^{2+} in all three experiments. (G-19)·(C-56) links the TΨC loop to the D-loop, forming the corner of the L structure. One of the four strong Mg^{2+} binding sites is located near this base pair; here, Mg^{2+} is coordinated directly

to the phosphate oxygen of G-19 and through water molecules to the N-7 and O^6 of G-20, O^4 of U-59, and N-3 of C-60 (Hingerty et al., 1978); Zn^{2+} appears to bind at this site, displacing Mg^{2+} and altering the arrangement of the ligands (Rubin et al., 1983), possibly due to the direct chelation of N-7 and O^6 of G-20. We are unable to determine whether G-20 or U-59 is affected since neither residue gives rise to a peak in the imino proton spectrum.

Both (G-15)·(C-48) and (G-19)·(C-56) are invariant base pairs that are important in stabilizing tertiary folding in tRNA. The imino protons of these base pairs have been shown to be sensitive to the paramagnetic divalent cations Co^{2+} and Mn^{2+} (Hurd et al., 1979). The Mg^{2+} binding site near G-19 is also a Pb^{2+} binding site. The hydrated Pb^{2+} ion appears to catalyze the alkaline hydrolysis of the polynucleotide backbone at positions 17 and 18, both dihydrouridine residues (Sundaralingam et al., 1984; Brown et al., 1985). Preliminary experiments in this laboratory suggest that at neutral pH Zn^{2+} ions can also facilitate the cleavage of tRNA at this site (unpublished data). These observations strongly suggest that Zn^{2+} can bind to at least two sites on the tRNA, one near (G-15)·(C-48) and the other near (G-19)·(C-56).

In the absence of Mg^{2+}, Zn^{2+} affects the imino proton resonances of base pairs U·A-12 and G·C-10 in both $tRNA^{Phe}$ and $tRNA^{Val}$. However, the presence of 1–2 strongly bound Mg^{2+} ions "protects" these resonances from Zn^{2+} (Table II). Both U·A-12 and G·C-10 are located near the Mg^{2+} site in the P-10 loop (Hingerty et al., 1978). The Mg^{2+} at this site is coordinated to the phosphate oxygens of U-8, A-9, and C-11. The effect of Zn^{2+} on these resonances may be due to the tetrahedral geometry of the Zn^{2+} complex as compared to the octahedral Mg^{2+} complex (Rubin et al., 1983). In solution the affinity of Zn^{2+} for this site appears to be less than that of Mg^{2+}.

In contrast to the imino protons of U·A-12 and G·C-10, the N1-H proton of Ψ-55 and the imino proton of (U-8)·(A-14) are only affected by Zn^{2+} when Mg^{2+} is present (Table II). The changes in chemical shift of the N1-H proton of Ψ-55 (resonance peak X, Figures 4–7) are probably due to the presence or absence of a hydrogen-bonded water molecule (Tropp & Redfield, 1981). In the hydrogen-bonded state peak X resonates at ~11 ppm, and when the interaction is disrupted, it shifts upfield to ~10.5 ppm (Tropp & Redfield, 1981; Heerschap et al., 1983b). The (U-8)·(A-14) base pair, which is involved in a tertiary interaction, links the base of the acceptor stem to the D-stem and anchors the elbow of the L structure. The effects of Zn^{2+} on these resonances may be indirect; binding of Zn^{2+} to the tRNA displaces one more Mg^{2+} which can now bind to other sites on the tRNA. The site or sites of Mg^{2+} interaction that lead to these effects are unknown. Two possibilities are (a) the site where Mg^{2+} is coordinated to the phosphates of G-20 and A-21 (Hingerty et al., 1978; Quigley et al., 1978) and (b) the site where Mg^{2+} coordinates to the phosphate oxygens of A-14 and G-57.

Zn^{2+} affects both yeast $tRNA^{Phe}$ and *E. coli* $tRNA^{Val}$ in much the same manner (Table II). However, there are at least two differences between these tRNAs. Peak W′ in yeast $tRNA^{Phe}$ is affected by Zn^{2+} while Y′, the equivalent resonance in *E. coli* $tRNA_1^{Val}$, is not. Peak W′ has been assigned to the amino proton of A-9 that is involved in the tertiary base triple (U-12)·(A-23)·(A-9) (Choi & Redfield, 1985). Since the NOE connectivities of peak Y′ in $tRNA_1^{Val}$ (Hare et al., 1985) are similar to those of W′ in $tRNA^{Phe}$, we conclude that Y′ is also due to the amino proton of A-9. The reason for the lack of a Zn^{2+} effect on this resonance in $tRNA_1^{Val}$ is unknown.

Table III: Comparison of Mg[a] and Zn[b] Binding Sites in $tRNA^{Phe}$

Zn^{2+}		Mg^{2+}	
ligand	coordination	ligand	coordination
Zn(1)	N-7 (G-20)	Mg(3)	N-7 (G-20)
	O^6 (G-20)		O^6 (G-20)
	O2P (G-19)		O2P (G-19)
	O^4 (U-59)		O^4 (U-59)
			N-3 (C-60)
Zn(2)	O2P (U-8)	Mg(1)	O2P (U-8)
	O2P (A-9)		O2P (A-9)
	O1P (C-11)		O1P (C-11)
	O2P (C-11)		
	O1P (U-12)		O1P (U-12)
		Mg(2)	O2P (G-20)
			O1P (A-21)
		Mg(4)	O2P (A-14)
			O2P (G-57)
Zn(3)	N-7 (G-15)		
	O^6 (G-15)		
	O^4 (U-8)		
	O1P (A-14)		
Zn(4)	N-7 (G-65)		
	O^6 (G-65)		
	O^6 (A-64)		
	N-7 (A-64)		
Zn(5)	N-7 (G-43)		
	O^6 (G-43)		
	N-7 (G-42)		
	O^6 (G-42)		

[a] Hingerty et al., 1978. [b] Rubin et al., 1983.

However, it does appear that the effect of Zn^{2+} on the two components of the base triple, U·A-12 and (A-23)·(A-9), is independent in $tRNA_1^{Val}$ since peak C, U·A-12, is affected by Zn^{2+} while A-9 is not and in $tRNA^{Phe}$, which contains 1–2 Mg^{2+} per tRNA, Zn^{2+} affects only peak W′, (A-23)·(A-9).

One effect of Zn^{2+} that is unique to $tRNA_1^{Val}$ is the upfield shift of the resonances associated with G·C-1 and G·C-2. These resonances are the terminal base pairs in the acceptor stem. Zn^{2+} may affect these resonances independently, since G·C-2, a component of peak NO, appears to be affected only at concentrations above 4 mM while G·C-1 is affected at all Zn^{2+} concentrations (Figure 2). This would appear to rule out the possibility that Zn^{2+} binds to these adjacent guanines by chelation of their N-7 and O^6 positions. At present the cause of these effects is unknown.

From the crystal structure of yeast $tRNA^{Phe}$ in the presence of Zn^{2+}, five Zn^{2+} binding sites were observed, two of which directly replace previously bound Mg^{2+} (Table III) (Rubin et al., 1983). From these data it appears that Zn^{2+} binds preferentially at the N-7 and O^6 positions of purine, in particular to adjacent purines located in the major groove of helical regions. The authors noted that, due to the geometry of Zn^{2+} complexes (tetrahedral) and to the preference of Zn^{2+} for sites on the bases, the arrangement of the ligands at these sites differs substantially from that of those bound to Mg^{2+}. The exact nature of these differences was not elaborated.

The potential binding sites that we have observed in solution [near (G-19)·(C-56), the P-10 loop, and (G-15)·(C-48)] correspond quite well to the zinc binding sites Zn(1), Zn(2), and Zn(3) of Rubin et al. (1983). In this study we did not observe changes in the imino proton spectra corresponding to zinc sites Zn(4) and Zn(5); however, with UV difference spectroscopy, binding sites of this type were observed (J. M. Flanagan, E. H. Lee, and K. B. Jacobson, unpublished information). One difference between the imino proton NMR spectral data and the crystal data is that Zn(2), which binds in the P-10 loop, can displace Mg^{2+} in the crystal, but not in solution. Further investigation will be required to obtain a

detailed understanding of the effects of Zn^{2+} on the molecular structure of tRNA.

ACKNOWLEDGMENTS

We express our gratitude to Dr. Brian Reid, University of Washington, for his generous permission to perform these experiments in his facilities and to him and Dr. D. Hare for stimulating and critical discussions.

Registry No. Zn, 7440-66-6.

REFERENCES

Arter, D. M., & Schmidt, P. G. (1976) *Nucleic Acids Res. 3*, 1437–1447.
Brown, R. S., Dewan, J. C., & Klug, A. (1985) *Biochemistry 24*, 4785–4801.
Butzow, J. J., & Eichhorn, G. L. (1975) *Nature (London) 254*, 358–359.
Choi, B. S., & Redfield, A. G. (1985) *Nucleic Acids Res. 13*, 5249–5254.
Farkas, W. R. (1968) *Biochim. Biophys. Acta 155*, 401–409.
Flanagan, J. M., & Jacobson, K. B. (1987) *J. Chromatogr. 387*, 139–154.
Hare, D. R., & Reid, B. R. (1982) *Biochemistry 21*, 1835–1842.
Hare, D. R., Ribeiro, S., Wemmer, D. E., & Reid, B. R. (1985) *Biochemistry 24*, 4300–4306.
Heerschap, A., Haasnoot, C. A. G., & Hilbers, C. W. (1982) *Nucleic Acids Res. 10*, 6981–7000.
Heerschap, A., Haasnoot, C. A. G., & Hilbers, C. W. (1983a) *Nucleic Acids Res. 11*, 4483–4499.
Heerschap, A., Haasnoot, C. A. G., & Hilbers, C. W. (1983b) *Nucleic Acids Res. 11*, 4501–4520.
Hiatt, V. S., & Jacobson, K. B. (1980) *Toxicol. Appl. Pharmacol. 56*, 116–126.
Hingerty, B., Brown, R. S., & Jack, A. (1978) *J. Mol. Biol. 124*, 523–534.
Hurd, R. E., Azhderian, E., & Reid, B. R. (1979) *Biochemistry 18*, 4012–4017.
Hyde, E., & Reid, B. R. (1985a) *Biochemistry 24*, 4315–4325.
Hyde, E., & Reid, B. R. (1985b) *Biochemistry 24*, 4307–4314.
Quigley, G. J., Teeter, M. M., & Rich, A. (1978) *Proc. Natl. Acad. Sci. U.S.A. 75*, 64–68.
RajBhandry, U. L., & Chang, S. H. (1981) *J. Biol. Chem. 243*, 598–608.
Redfield, A. G. (1978) *Methods Enzymol. 49*, 253–261.
Reid, B. R. (1981) *Annu. Rev. Biochem. 50*, 969–996.
Reid, B. R., McCollum, L., Ribeiro, N. S., Abbate, J., & Hurd, R. E. (1979) *Biochemistry 18*, 3996–4005.
Roy, S., & Redfield, A. G. (1983) *Biochemistry 22*, 1386–1390.
Roy, S., Papastavros, M. Z., Sanchez, V., & Redfield, A. G. (1984) *Biochemistry 23*, 4395–4400.
Rubin, J. R., Wang, J., & Sundaralingam, M. (1983) *Biochim. Biophys. Acta 756*, 111–118.
Sundaralingam, M., Rubin, J. R., & Cannon, J. F. (1984) *Int. J. Quantum Chem. 11*, 355–366.
Tropp, J. S., & Redfield, A. G. (1981) *Biochemistry 20*, 2133–2140.
Werner, C., Krebs, B., Keith, C., & Dirheimer, G. (1976) *Biochim. Biophys. Acta 432*, 161–175.
Wintermeyer, W., & Zachau, H. G. (1973) *Biochim. Biophys. Acta 299*, 82–90.
Wong, Y. P., Reid, B. R., & Kearns, D. R. (1973) *Proc. Natl. Acad. Sci. U.S.A. 70*, 2193–2195.

24,26-Dihydroxyvitamin D_2: A Unique Physiological Metabolite of Vitamin D_2†

Nicholas J. Koszewski,‡ Timothy A. Reinhardt,§ Joseph L. Napoli,‖ Donald C. Beitz,‡ and Ronald L. Horst*,§

Department of Biochemistry and Biophysics, Iowa State University, Ames, Iowa 50011, The Mineral Metabolism and Mastitis Research Unit, National Animal Disease Center, Agricultural Research Service, U.S. Department of Agriculture, P.O. Box 70, Ames, Iowa 50010, and Department of Biochemistry, State University of New York, Buffalo, New York 14214

Received December 1, 1987; Revised Manuscript Received April 14, 1988

ABSTRACT: A new vitamin D_2 metabolite, 24,26-dihydroxyvitamin D_2, has been detected in the plasma of rats fed physiologic amounts of vitamin D_2. The identity of the new metabolite (isolated from cow plasma) was established by ultraviolet absorbance, mass spectroscopy, chemical reactivity, and NMR spectroscopy. Among these, the mass spectrum was unique for the presence of a peak at M – 48 that was attributed to an intramolecular rearrangement involving both the C-24 and C-26 hydroxyl groups. A 300-MHz ^1H NMR spectrum of 40 μg of metabolite indicated a downfield shift of the C-28 methyl group signal to δ 1.30 and a multiplet at δ 3.66 corresponding to the hydroxylated C-26 methyl group. We determined that the formation of 24,26-dihydroxyvitamin D_2 represented a major pathway for further metabolism of 24-hydroxyvitamin D_2 in rats, exceeding the formation of 24,25-dihydroxyvitamin D_2. Standard bioassays revealed that 24,26-dihydroxyvitamin D_2 possessed very little biological activity and most likely represents a deactivation pathway for 24-hydroxyvitamin D_2.

The metabolism of vitamin D_3 has been extensively characterized and largely consists of oxidative modifications occurring in the side chain (Horst et al., 1983; Jones et al., 1983, 1984; Napoli & Horst, 1982; Napoli et al., 1982; Norman, 1984; Tanaka et al., 1981; Wichmann et al., 1981). The metabolism and biological activity of vitamin D_2 are generally thought to parallel those of vitamin D_3, and as such, it is freely administered to both humans and commercially important mammals (DeLuca, 1978; Norman, 1979). As a result, vitamin D_2 is prescribed for patients with a wide variety of

† This is Journal Paper No. J-12703 of the Iowa Agriculture and Home Economics Experiment Station, Ames, IA, Project No. 2504.
* Author to whom correspondence should be addressed.
‡ Iowa State University.
§ U.S. Department Of Agriculture.
‖ State University of New York.